

Aerosol Assisted Dielectric Barrier Discharge Plasma Jet for PMMA/ZnS Nanocomposite Thin Films Preparation

Mohaned A. Abed

Department of Physics- College of Science- University of Thi-Qar

Email: mohaned.ali88@yahoo.com

Mobile: 964 7802867731

Abstract:

Pure Poly methyl methacrylate (PMMA) thin films and PMMA mixed with 1 %, 3%, 5% &7% by weight of ZnS nanoparticles (NP) were prepared by plasma jet technique. Formulation of the polymer with nanoparticles allows for modification of polymer physical properties. The PMMA /ZnS nanocomposite prepared by polymerization in plasma jet and characterized by Ultra Violet Visible UV-Vis, Fourier Transform Infra-Red Spectrophotometer (FTIR), Atomic Force Microscopy (AFM) and SEM to study the effect of ZnS nanoparticles on the optical properties, morphology and structure of the thin films. The FTIR spectra for the films show an interaction between PMMA and NPs. There is a decrease in the optical band gap of films prepared with an increase of the concentration of NPs. AFM and SEM images show that there are a few clusters of ZnS and there is a homogeneous distribution of the nanoparticles in the PMMA matrix.

Keywords: ZnS Nanoparticles, Nanocomposite, Thin films, FTIR, Structure properties.

Introduction:

In several last year plasma polymers containing small metal, particles have been studied due to their novel physical properties and hopeful application. Plasma is often done by wherewithal of a dielectric barrier discharge. This is mostly Achieved through a parallel plate electrode system. At least one of the electrode surfaces is covered with a dielectric. For creating the discharge a gas is brought between the two electrodes to be ionized. Inert gasses like argon, helium, and nitrogen commonly used carrier gasses[Topala et. al., 2008]. Most often gasses and aerosols are used. In this work aerosols will be use and the technique was the atmospheric plasma jet deposition. Molecular particles can split up by plasma. Only elements and components with a low molecular weight can be utilized as the gas precursor in plasma depositing applications. As there are much more liquid precursors available than gaseous, the number of possible material is apparently higher when working with aerosol precursors. Various nanoparticles and monomer systems can be simultaneously applied in

aerosol form during plasma treatment. So working with aerosol precursors offers more flexibility [Tota Pirdo Kasih, 2007]. Various techniques can be used to product aerosol: nozzles and ultrasonic piezoelectric technology. Various techniques can be used to produce aerosol: ultrasonic piezoelectric and nozzles. The nozzles are a most stable system in continuous production. Smaller size reduction, high precursor plasma interaction [Van Hove et. al., 2007]. Special nozzle was used in this work to produce an aerosol. One of the major defiance in the preparation of high-performance polymer/not - metallic particle composite thin films and succeed a homogeneous dispersion of nanoparticles in the polymer. Because the good dispersion of nanoparticles in a polymer matrix this criterion is lifeline[Giannelis, 1996]. The in-situ polymerization it was used in this work, in the polymerization process for the preparation of the PMMA/Fe₂O₃ nanocomposite thin films. PMMA selected from among different polymers due to the simple synthesis procedures, environmental stability and good thermal [Vodnik et. al.,2009]. The impetus

behind this inspection is to examine the characteristic change in the optical properties of PMMA when they are embedded Fe₂O₃ nanoparticles in that part. Here PMMA plays the role of an mediator dielectric medium. These nanoparticles are best suitable for the application in photonics, photography, enhanced surface Raman scattering, and surface enhanced fluorescence, catalysis, data storage, laser random etc [Jin et. al., 2001]. Therefore the synthesis of PMMA–ZnS nanoparticle composite is receiving wide attention.

Experimental Details:

Dielectric barrier discharge system (DBD) plasma jet used in thin film deposition is composed of the high alternating voltage power supply, generates a high voltage of sinusoidal shape of 7.5 kV peak to peak the frequency of 28 kHz, the plasma jet torch, gas supply and fitting. The non thermal atmospheric pressure plasma torch shows in Fig.1. ZnS nanoparticles average particle size was 40 nm and purity of 99.9%. Different concentration of nanoparticles (1%, 3%, 5%, and 7wt%) was mixed with Methyl Methacrylate Monomer (PMMA). The mixing up dispersed by ultrasonic to ensure a homogeneous distribution of nanoparticles, then PMMA/ZnS nanocomposite thin films deposited by DBD plasma jet system on a ultrasonically cleaned glass substrate of standard size 10 x 10 mm. Fig.2 submit a photograph for the non-equilibrium atmospheric pressure plasma system for PMMA/ZnS nanocomposite thin films productions. The mixture (PMMA/ZnS) convert into an aerosol when argon gas was passed through a nebulizer, which contains a mixture.

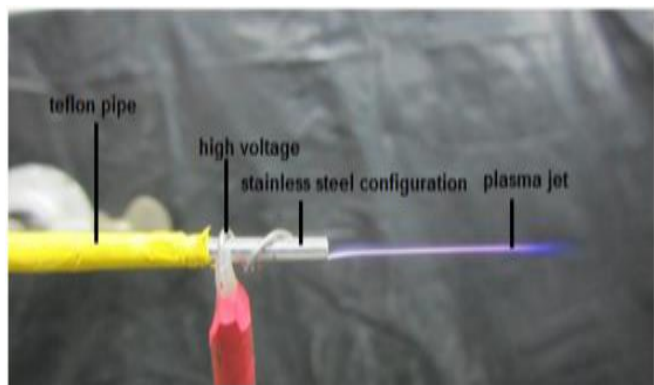


Figure (1) Photograph at working of the non-thermal atmospheric pressure plasma torch

For measuring UV-Visible absorption spectra of pure PMMA and PMMA/ZnS nanocomposite thin

films adouble beam UV-VIS-NIR210A Spectrophotometer was used. Thin films surface morphological analysis is carried out by SEM and the structure analysis is achieved by X-ray diffractometer system kind SHIMADZU 6000. To calculate thickness of the films the optical interferometry method was used.

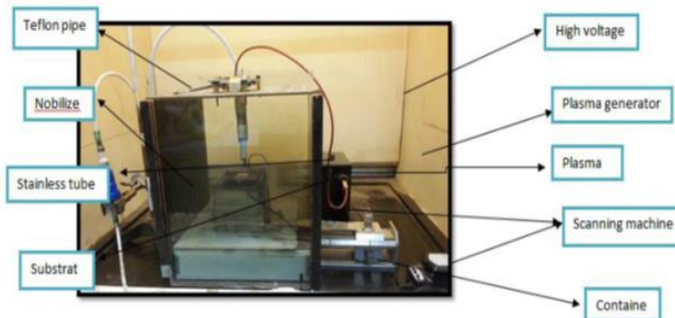


Figure (2) Photograph for the non-equilibrium atmospheric pressure plasma system for PMMA/ZnS nanocomposite thin films preparations

Results and Discussion:

Absorption Spectrum:

The absorption spectrum shows fig.3 for PMMA/ZnS thin films with the different concentrations of ZnS nanoparticles that is (1,3, 5, and 7wt%) as well as the pure PMMA thin films. Table 1 shows the thickness of thin films for pure PMMA and every concentration. Pure PMMA film has peaked at 294 nm and when the concentration of ZnS nanoparticles increase the thin films for PMMA/ZnS nanocomposite shifted towards long wavelength.

Absorption Coefficient:

Fig.4 shows the absorption coefficient of PMMA/ZnS nanocomposite for four concentrations and pure PMMA computed by the equation [Wasan et. al., 2014]

$$\alpha = 2.303 A/t \dots (1)$$

Where A the absorbance and t the thickness.

Table (1) The experimental condition for the preparation of pure PMMA thin film and PMMA/ZnS nanocomposite thin films samples thickness (nm)

Sample	Thickness (nm)
Pure PMMA	267
ZnS 1wt%	250
ZnS 3wt%	289
ZnS 5wt%	250
ZnS7wt%	280

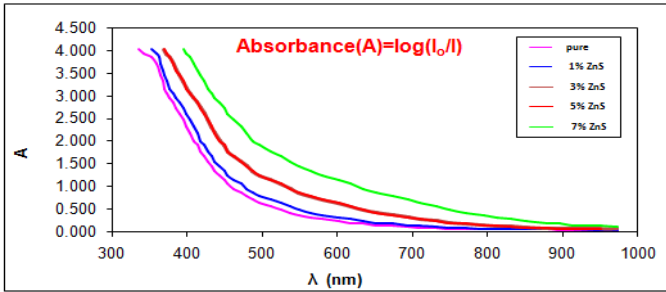


Figure (3) Absorption spectrum for pure PMMA and PMMA/ZnS nanocomposite 1, 3, 5, and 7wt% ZnS NPs

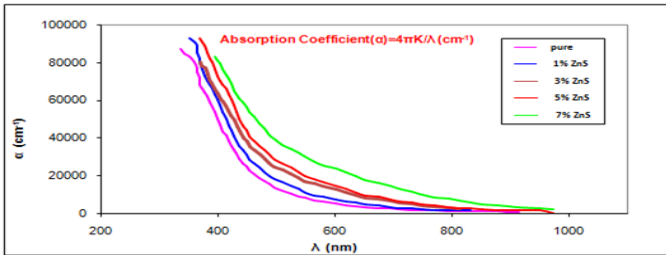


Figure (4) Absorption coefficient for pure PMMA and PMMA/ZnS nanocomposite 1, 3, 5, and 7wt% ZnS NPs

Optical energy band gap:

Fig.5 explain the optical energy band gap It has been determined by plotting the dissimilarity of $(\alpha h\nu)^2$ versus (eV) for direct energy gap transition. When the ZnS NPs concentration increased this lead to reduce of E_g from 1.7 eV for 7wt% ZnS concentration to 1.9 eV for 5wt% ZnS concentration to 1.98 eV for 3wt% ZnS concentration to 2.0 eV for 1wt% ZnS concentration while for pure PMMA film was 2.38 eV. The modification of polymer structure cause reduce in energy gap and also the addition of NPs to polymer induces a structural ordering of the polymers and these changes are supporting by UV-Vis spectra, so the optical band gaps vary with ZnS concentration.

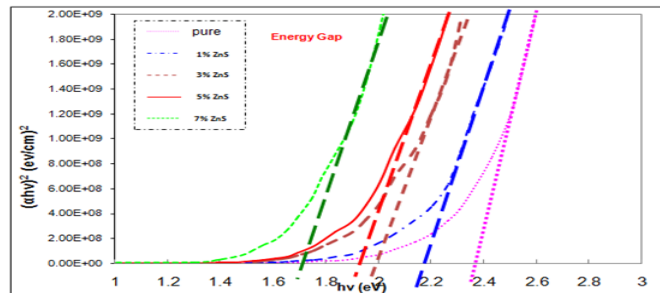


Figure (5) The E_g for pure PMMA film, 1 wt.% ZnS concentration, 3wt.%, 5wt.% and 7% wt.% all at constant gas flow rate 1L/min.

Fig.6. shows the variation of refractive index calculated from the relation [8]

$$n = \left(\frac{4\pi}{1-R} - k^2 \right) + \frac{(1+R)}{(1-R)} \dots (2)$$

Where

R (the reflectance and the annihilation coefficient) with wavelength for pure PMMA and PMMA/ZnS nanocomposite thin films at the four of ZnS NPs, the increasing in ZnS NPs concentration lead to increment in refractive index.

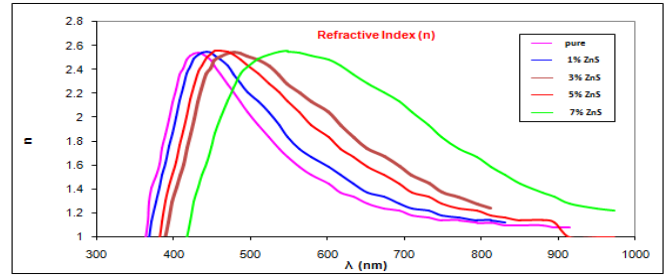


Figure (6) The variation of the refractive index (n) with wavelength for pure PMMA film, 1wt.% ZnS concentration, 3wt.%, 5wt.% and 7% wt.%

X-Ray Diffraction:

The XRD pattern for pure PMMA thin film shows in Fig.7. The figure demonstrates that the X-beam diffraction showed that the thin films have an amorphous structure. Plasma polymer has short chains of building units and a high degree of cross-linking. Plasma polymers are amorphous in nature, where contain of short chains of monomers have a high degree of cross-linking.

Fig.8 for PMMA/ZnS nanocomposite films at ZnS NPs concentration 5 and 7wt%, for pure PMMA the film has an amorphous structure. Four main peaks presented the reflections which are assigned to the lattice planes 111, 020, 202 and 311.

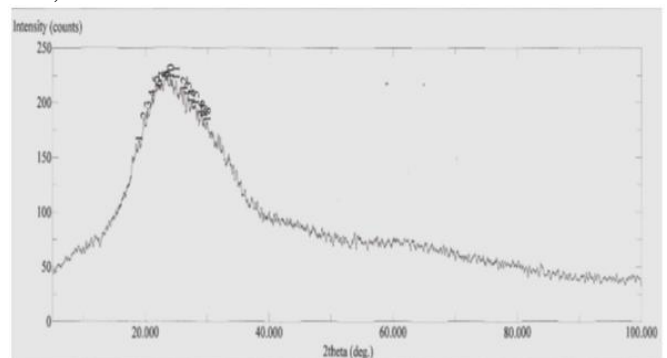
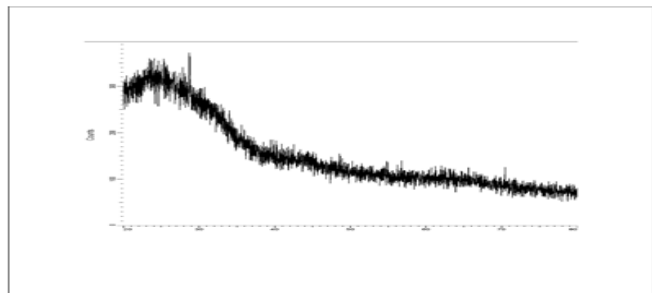
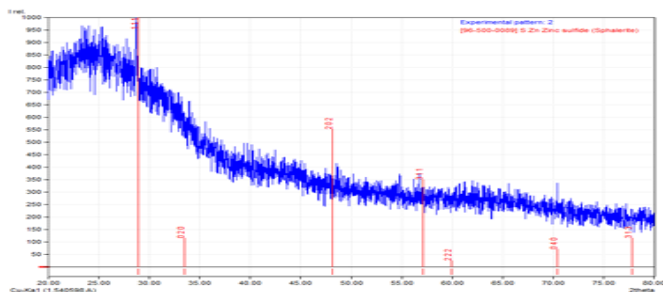


Figure (7) XRD for pure PMMA thin film



a



b

Figure (8) XRD (a) for PMMA/ZnS nanocomposite film at 5wt.%
(b) PMMA/ZnS nanocomposite film at 5wt.%

Scanning Electron Microscope:

The shape and distribution of ZnS NPs were found by performing scanning electron microscopy. The SEM image of PMMA/ZnS nanocomposite thin film shows in fig.9 at 7wt% PMMA/ZnS NPs concentration. The SEM images indicate that ZnS NPs disperse in the PMMA matrix with a relatively uniform distribution and formed some clusters of NPs. The ZnS nanoparticles are homogeneously dispersed in the polymer matrix.

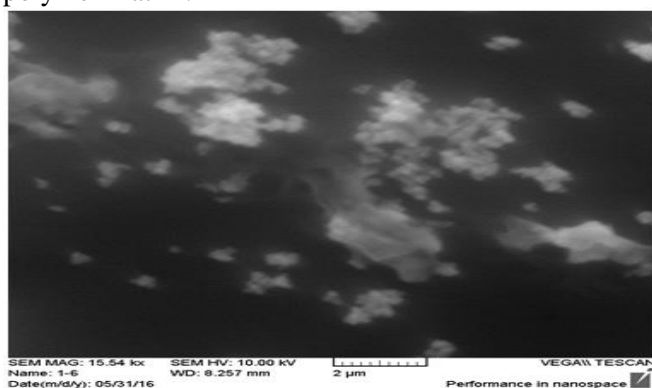


Figure (9) SEM image for PMMA/ZnS nanocomposite film at 7wt.% ZnS NPs concentration

Atomic Force Microscopy of PMMA/ZnS:

The morphological characteristics of the PMMA/ZnS nanocomposite thin films have been studied by atomic force microscope (AFM) to monitor the structure under the influence of addition of ZnS nanoparticles with 7wt%. Concentration, and compare it with the surface roughness of pure polyaniline thin film. Two and three-dimensional AFM images of the PMMA/ZnS thin film of (7wt%.Zn) is shown in figure (10). It is found that the surface roughness average particle diameter is 87.85nm, while for PMMA/ZnS thin film.

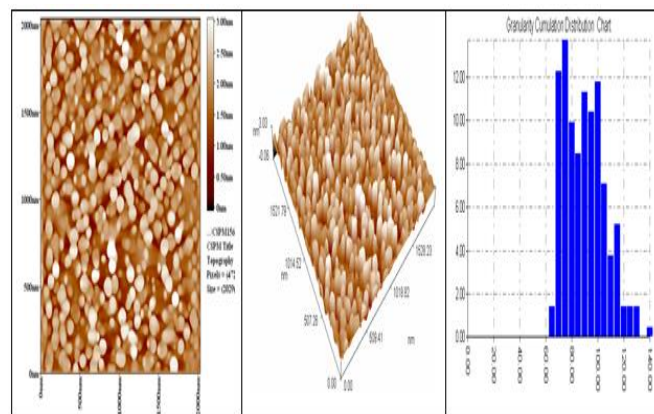


Figure (10) AFM photographs of PMMA/ZnS thin film at 7wt.% ZnS: 2D image, 3D image and granularity accumulation distribution chart

Conclusions:

A new material with a different chemical structure made by the preparation of nanocomposite films by plasma polymerization. An imitative polymer has high cross-linked, high density and highly branched and this different from polymer polymerized by plasma, as a result, this influence on the linear refractive index appear. The ZnS particles are uniformly distributed in the PMMA matrix. The optical energy bandgap decreased When the weight percentage of the ZnS increased in the nanocomposite thin films, and the structure of polymer modifies.

References:

- Giannelis E.P., "Polymer layered silicate nanocomposites", Advanced Materials, 8 29-35., 1996.
- Jin R.C., Cao Y.W., Mirkin C.A., "Photo Induced Conversion of Silver Nanospheres to Nanoprisms", Science 294, 1901, 2001.

- Topala I., Asandulesa M., Dumitrascu N., Popa G., Durand J., "Application of Dielectric Barrier Discharge for Plasma Polymerization Processes", *Journal of Optoelectronics and Advanced materials*, 10, 2028 – 2032, 2008.
- Tota Pirdo Kasih, "Development of Novel Potential of Plasma Polymerization Techniques for Surface Modification", Gunma University, Thesis for The Degree of Doctor of Engineering, (2007).
- Van Hove, Tom *Tweemaandelijks Tijdschrift Voor de Textielindustrie*, "Depositing micro- and nano-sized coatings by means of Aerosol assisted large area cold atmospheric", *Plasma Technology*, 15, 4, 38-47, 2007.
- Vodnik V.V., Božanić D.K., Džunuzović E., Vuković J., Nedelj ković J.M., "Thermal and Optical Properties of Silver Poly(methylmethacrylate) Nanocomposites Prepared by insitu Radical Polymerization", *European Polymer Journal*, 64, 1-22, 2009.
- Wasan Al-Taa'y, Mohammed Abdul Nabi, Rahimi M. Yusop, Emad Yousif, Bashar, Mudhaffar Abdullah, Jumat Salimon, Nadia Salih, and Saif Ullrwan Zubairi, "Effect of Nano ZnO On the Optical Properties of Poly(vinyl chloride) Films", *International Journal of Polymer Science*, 2014, 1-6, 2014.